COBEM 2021 26th International Congress of Mechanical Engineering
November 22-26, 2021, Virtual Congress, Brazil
ABCM Associação Brasileira de Engenharia e Ciências Mecânicas

COB-2021-0013
MECHANICAL VIBRATION EFFECTS IN THE BIOSPECKLE LASER TECHNIQUE FOR PORTABLE EQUIPMENT APPLICATION

Daniel Bernardes de Castro
Technological Institute of Aeronautics - Praça Marechal Eduardo Gomes, 50, Vila das Acácias, 12228-900, São José dos Campos/SP
danieldbc@ita.br

José Eduardo Silva Gomes
Roberto Alves Braga Jr.
Henrique Leandro Silveira
Federal University of Lavras - Campus Universitário, 37200-900, Lavras/MG
jose.eduardo@varginha.com.br; robertobraga@ufla.br; henrique.silveira@ufla.br

Abstract. *The biospeckle laser (BSL) is a technique developed based on the processing of optical interference patterns formed when a laser light strikes a biological surface. This non-destructive image processing technique is used to quantify the activity level of a sample. Since it is not always feasible to move biological samples to a laboratory to be analyzed, on-site application is necessary for the advancement of the technique. There are limitations in the use of the technique in the field, vibration interference is one of them. Aiming to understand the level of this interference as well as to propose ways to mitigate them, in this work it was developed a portable prototype for dynamic laser speckle (DLS) analysis that was subjected to experimental modal analysis and transmissibility tests. The prototype's natural frequencies were obtained and it was evaluated how the optical technique behaves when excited at these and other frequencies. It was discovered that BSL is more sensitive to low frequencies, close to 5 Hz. In the transmissibility tests, it was found that the isolator with the lower stiffness presented the best characteristics of vibration isolation for the proposed purposes, making possible the portability of the prototype from the isolation of ordinary external mechanical vibrations.*

Keywords: *dynamic speckle, portability, vibration, modal analysis, transmissibility.*

1. INTRODUCTION

The speckle laser is an optical interferometry phenomenon that occurs when a material is illuminated by a laser and it has been adapted as a sensitive tool for detecting changes in biological surfaces (Rabal and Braga, 2008). As it is a non-destructive, non-invasive, and low-cost technique, it has become very advantageous for studies in various areas of knowledge such as biology, agronomy, and bio-medicine. When applied to dynamic surfaces, such as paint drying, for example, a continuous formation of new and different optical interference patterns is observed, and this random and dynamic pattern is called dynamic laser speckle (DLS) or biospeckle laser (BSL), if the surface in question is of biological origin, as in plants and bacteria.

Visually, this variation of the optical interference pattern over time can be compared to a boiling liquid or the image in television far from tuning, where light grains correspond to constructive interference and dark grains to destructive ones (da Silva, 2007). This granular dynamic pattern carries information about the illuminated surface (Fracarolli, 2011). In fresh paint, the seething of this pattern, which can also be associated with activity, is greater than in dry paint, for example.

Several works with significant results have been published involving analyzes of seeds (Braga *et al.*, 2001) and fruits (Ansari and Nirala, 2013; Blotta *et al.*, 2009), blood flow (Aizu and Asakura, 1991), parasite activities (Pomarico *et al.*, 2005), motility of bovine semen (Carvalho *et al.*, 2009) etc. All of them were performed in a laboratory environment with complex setups.

Various bench equipment is now available in more compact versions, enabling portability and/or saving space. Making it possible to transport them to more remote areas, allowing the equipment to go to the sample to be analyzed. They can be cheaper and simpler to use than conventional bench instruments. However, when reducing the size of a device, there may also be a reduction in its sensitivity, depending on the detection limit to be evaluated (McMahon, 2008).

The works that propose the portability of the biospeckle laser in the scientific literature are scarce and recent. This is due to the fact that the technique is relatively new compared to other optical methods, such as shearography (a standardized technique where there is already numerous commercial equipment). Furthermore, it is a technique that is very sensitive to external noise, such as vibration.

Speckle interferometry techniques, such as digital shearography and digital speckle pattern interferometry, which are

optical methods used to measure deformations in bodies, suffer from several inconvenient effects that can generate high levels of noise and errors in experimental measurements. Much of this noise originates from external disturbances, such as vibration (Lopes *et al.*, 2017). Vibration in instrument panels may cause meter malfunction or difficulty reading (Rao, 2010). Electronic components used in automobiles, aircraft, machines, etc. may also fail due to vibration (Inman, 2007).

In the scientific literature, no studies were found in order to evaluate and attenuate the disturbance of the external vibration in the biospeckle laser. Due to the need to expand the technique beyond optical laboratories, this work proposes to evaluate one of the main factors that can compromise the reliability and hinder the portability of the technique: the interference of mechanical vibration.

To quantify this vibration, a portable BSL equipment was developed, in which the frequencies and magnitudes of vibration that can interfere with the technique were investigated, through experimental modal analysis. Vibration transmissibility tests were also carried out to evaluate the efficiency of vibration attenuation promoted by 11 different vibration isolators.

2. MATERIAL AND METHODS

2.1 Materials

In this work, the tests that were carried out aimed to quantify the interference of external noise in the DLS under different conditions of excitation and isolation, thus evaluating the feasibility of the portability of the technique. They are experimental modal analysis, dynamic laser speckle, and transmissibility. Camera, laser, and PC, together with SpeckleTool and Octave software form the configuration for performing biospeckle laser or dynamic laser speckle analysis. Shaker, accelerometers, load cell, power supply, and dynamic analyzer form the configuration for performing the experimental modal analysis. Transmissibility was obtained using the shaker, 2 accelerometers, and dynamic analyzer.

2.2 Prototype design and validation

To carry out the tests proposed in this work, a compact and portable prototype equipment was developed to perform the dynamic laser speckle tests. This equipment contains the camera and laser fixed to a base of raw MDF wood, with dimensions 22.8 x 21.5 cm and height 1.5 cm, by means of metal rods characteristic of optical experiments (Figure 1a).

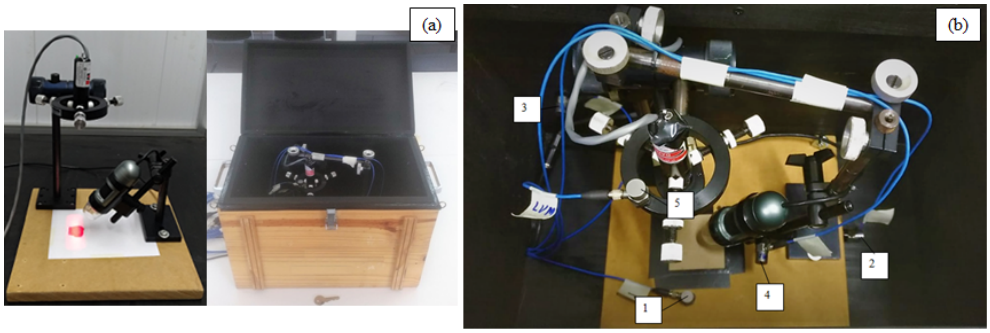

Figure 1. Prototype - Compact experimental setup (a); Positions of accelerometers on the prototype (b).

Due to the interference of external light in the technique, the wooden base with the screwed devices was enclosed in a wooden box, with a base of dimensions 41 x 23.8 cm and height 29.5 cm, in order to nullify any kind of interference that external light may cause in the measurements, as shown in Figure 1a. The total mass of the equipment is 5.3 kg.

For a better resolution of the processed image packages, it is interesting that the camera sits as close as possible to the sample. When defining the distance of the laser to the sampled surface, it was decided to leave it at a distance of 7.5 cm. The distance was experimentally defined, where the maximum aperture of the laser beam can illuminate the entire sampled region (≈ 500 mm^2) without the need for an expander lens. To obtain a satisfactory image saturation, a filter lens was also used between the laser and the sample, to attenuate its intensity.

One of the most used forms of validation of the DLS technique is through ink drying analysis, because, in addition to being a technique replicated several times in the scientific literature for validation of experimental configurations and analysis methods, results can be compared via a precision scale (Junior *et al.*, 2007; Chaves, 2011; Pra *et al.*, 2009; Zhong *et al.*, 2013). The results of this validation can be seen in de Castro (2020).

2.3 Obtaining the prototype's natural frequencies

The first vibration test performed was the experimental modal analysis, to obtain the prototype's natural frequencies through the frequency response function (FRF), which is a measurement that involves two channels and that relates the

spectrum of channel 2 (output) with channel 1 (input). It measures the response of the system tested and its quality depends on the type of average used in the samples. In this work, the vector average was applied, used to reduce the noise level of the spectrum, in addition to improving the precision and repeatability of the experiment.

As the structure is complex and composed of several components, aiming at a better characterization of the system, five accelerometers (PCB model 352C33) were fixed inside the box, as shown in Figure 1b, to measure the vibration levels in each position: accelerometer 1 (AC1) → fixed to the side of the sample; accelerometer 2 (AC2) → attached to the side of the wooden base (x-axis); accelerometer 3 (AC3) → mounted on the box wall (y-axis); accelerometer 4 (AC4) → attached to camera bracket; accelerometer 5 (AC5) → attached to the laser holder.

Accelerometers 1 to 3 were positioned to capture vibrations in the 3 axes (x, y, and z) and accelerometers 4 and 5 were fixed to the camera and laser, the main components of the biospeckle laser analysis. The assembly conditions of the structure for performing the modal test can be classified in three ways: free-free, completely fixed, and assembled in the real installation (Avitabile, 2018). In this experiment, the free-free condition was used.

The box was suspended on a metal support by two 0.5 mm nylon wires through four hooks fixed on the sides of the box, thus simulating the free condition. Once suspended, the box was leveled with a spirit level, and the shaker, also suspended by a support, was fixed in three different positions at the box, on the x, y, and z-axis, in order to obtain the responses to excitations in these three axes (Figure 2a).

To laterally decouple the shaker (The Modal Shop, model K2007E01) from the tested structure, a connection device called stinger was used. At the end of the stinger, a load cell was fixed, which measures the force that the excitation source (shaker) applies to the box. According to Porcu *et al.* (2019), forces with low energy levels are already sufficient to stimulate responses in resonance. The load cell was powered by the Minipa source - MPL-3305M and connected to the signal analyzer (Stanford Research Systems (SRS) 2-channel dynamic signal analyzer, model SR785) on channel 1, representing the input signal. The simplified experimental setup can be seen in Figure 2b. Computer, signal analyzer, source, shaker and laser (635 nm Coherent SNF laser - which is inside the box) were fed by the 127 V electrical network. The data obtained by the SR785 analyzer were later transferred to the computer using a pen drive.

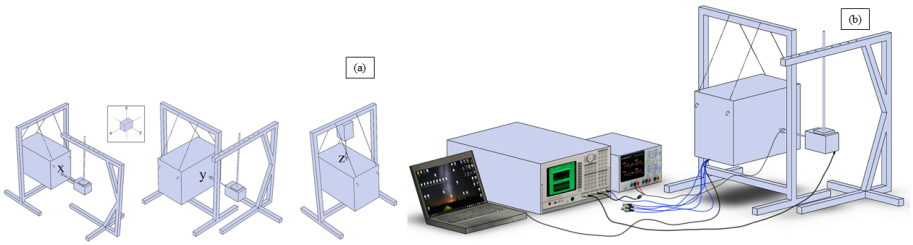

Figure 2. Axes orientation (a); Experimental setup for modal analysis (b).

With the setup aligned and adjusted, the configuration chosen for the shaker excitation was chirp with burst of 80% and amplitude of 40 mV, for the three axes. The excitation signal is generated by the SR785 dynamic analyzer that allows measuring the response of electronic, mechanical, and acoustic devices without the need for an external generator. It's an advantage when it comes to synchronization compared to an external source.

The chirp excitation is one of the most used in modal testing and offers a sinusoidal sweep of the same amplitude in each band of the selected spectrum. You can choose to scan from 0 to 50 Hz, from 0 to 1000 Hz, or from 100 to 200 Hz, for example. In practice, the excitation provokes through the shaker frequencies that go from low to high frequencies in a short interval. Each scan takes place within a sampling interval of the FFT analyzer (SR785). This form of excitation is useful for measuring frequency responses quickly, without having to make multiple discrete measurements using just a single sine wave. The FRF and the resulting coherence obtained are one of the best for linear systems and the technique is also used to identify non-linear features of the system (Avitabile, 2018).

For each axis, an FRF was obtained for each accelerometer, totaling 15 FRFs (3 axes and 5 accelerometers). In each scan in the selected frequency ranges, the signal analyzer (SR785) samples 800 points, that is, if a chirp scan from 0 to 800 Hz is configured, for example, we have 800 lines of discrete data (amplitudes) for each integer frequency from 0 to 800. In this work, in order to obtain a better data discretization, it was decided to perform 4 scans for each FRF.

It was observed in preliminary tests that the DLS suffered greater disturbances when excited at lower frequencies, up to approximately 200 Hz. As the camera's capture frequency is 15 fps, or 15 Hz, aiming at a more accurate observation of the phenomenon, it was opted for a greater sample discretization in this frequency range, as shown in Table 1.

The number of sweeps (scans) column represents the number of chirp pulses, in the respective excited frequency ranges, that were executed. The resulting FRF is represented by the averages of these 20 pulses.

As the chirp excitation scans from low to high frequency for each sample interval, the time response will amplify as the sweep passes through the natural frequencies. Thus, the peaks of the FRFs represent regions of resonance, where the prototype's natural frequencies are present.

Table 1. Frequency ranges and number of sweeps.

Excited frequency range for each accelerometer (x, y, and z axes)	Number of sweeps (averages)
0 - 25	20
0 - 200	20
200 - 600	20
600 - 1000	20

2.4 Dynamic laser speckle analysis by frequency and software used

Once the natural frequencies of the prototype were obtained, with it still suspended in the free-free condition, Figure 2b, a new frequency scan was made for each axis (x, y, and z), this time punctually and simultaneously with the dynamic laser speckle analysis, so that it was possible to analyze the DLS behavior through AVD (acronym for absolute value of the differences) which is the speckle laser numerical method adopted in this work, at frequencies from 0 to 1000 Hz.

For each punctual excitation in frequency, 3 captures of 128 images were taken by the camera simultaneously at 15 fps (to perform the DLS test by means of AVD), opting for a scan with the following discretizations: from 0 to 30 Hz $\rightarrow$ 1 in 1 Hz; from 30 to 50 Hz $\rightarrow$ 2 in 2 Hz; from 50 to 100 Hz $\rightarrow$ 5 in 5 Hertz; from 100 to 500 Hz $\rightarrow$ 10 in 10 Hertz; and from 500 to 1000 Hz $\rightarrow$ 25 in 25 Hz. Altogether, 999 captures were made, 333 per axis.

In this work, the software SpeckleTool version 1.2.3 was used to perform all image collections, which captures images in 8 bits, in grayscale with dimensions 640 x 480 pixels. The camera (Dino-Lite AM3013) communicated with the computer via a USB cable that runs through a small, sealed hole in the bottom of the case, along with the accelerometer and laser power cables. For image processing, the software GNU Octave version 4.4.0 was used, and the SR785 dynamic signal analyzer was used to generate the vibration signals.

In order to investigate the interference of vibration in the speckle dynamic laser or biospeckle technique, the numerical method of absolute value of the differences (AVD) was used, which is a dimensionless number that quantifies the overall activity level of the sample, and was obtained by processing the images in software Octave (Braga *et al.*, 2016).

2.5 Vibration evaluation under real conditions and transmissibility

In order to understand the behavior of the DLS technique and how it relates to the excitation frequency, the previous tests were performed under ideal conditions, that is, with the box suspended in free-free condition. However, it is necessary to evaluate the DLS behavior in real conditions of use for a portable device.

Tests were carried out with the prototype on a wooden table (160 x 68.5 x 76.5 cm) with the shaker exciting it at a distance of 30 cm from the prototype. The experimental setup is similar to Figure 3b, but without the shock absorber (in orange) under the prototype.

Since the behavior of the AVD, concerning frequency, was extensively explored in the previous section, and in order to optimize and make feasible the performance of the new tests, 8 point frequencies for excitation were strategically defined, to cover the entire frequency range from 0 to 1000 Hz. They are: 5, 15, 25, 42, 60, 112, 470 and 800 Hz. The frequencies 5, 15, and 25 Hz characterize low-frequency excitations, in the camera's capture frequency range, a region where the DLS was more sensitive. Frequencies 42, 60, and 112 Hz characterize medium frequency excitations, being regions where resonances occurred according to previously calculated FRFs. The frequencies of 470 and 800 Hz represent high-frequency excitations, a region where the DLS was less sensitive.

Aiming to investigate the influence of the excitation amplitude on the results, all excitations were performed at three different amplitudes: 40, 70, and 100 mVpk. The *pk* in the unit characterizes that the source amplitude (shaker) in millivolts (mV) is represented by the peak voltage, that is, by the maximum instantaneous value of the function from the zero volt level (SRS, 2017).

One way to assess the vibration isolation performance of a system is through vibration transmissibility, which can be interpreted as the level of vibration transmitted from one structure to another. Transmissibility tests were performed using two accelerometers. An input, located next to the shaker fixation point on the table, and an output, which is the accelerometer 1, positioned in the z-axis direction, beside the surface sampled by the DLS, inside the box, which remained positioned 30 cm away from the shaker (Figure 3b).

The transmissibility curves were obtained employing the dynamic signal analyzer SR785 in an analogous way to the FRF, that is, relating the output acceleration signal with the input acceleration signal, both obtained simultaneously by two PCB-352C33 accelerometers. The excitation that was promoted by the shaker was the chirp type, in the range from 0 to 200 Hz. It was not necessary to scan at longer intervals due to the evident drop in transmissibility for high frequencies, which was proven by preliminary tests. If transmissibility T_d>1, there is an amplification of the signal, that is, the response was greater than the input. If T_d<1, vibration attenuation occurs (Balbinot, 2001; Becker, 2006).

In this work, 11 types of mechanical isolators were investigated, Figure 3a. With the transmissibility curves, it was

possible to identify which of these devices are more efficient in attenuating the external mechanical vibration under the studied conditions.

Table 2 describes the shock absorbers as well as their specifications. In item 6, black rubber, two strips of this rubber were used at the ends along the largest dimension of the base of the box (41 cm). For the shock absorber (vibra-stop) and springs (both BOSCH brand), items 7, 8 and 9, 4 units of each were used, arranged at the ends of the base of the box. Regarding items 10 and 11, the prototype box was suspended on the table by means of the easel, as can be seen in Figure 3c. For foams and bubble wrap, they were arranged symmetrically under the box, as illustrated in Figure 3b.

Table 2. Shock absorbers used.

Item	Name	Code	General Specifications
1	Orange foam	ESPLAR	Dimensions 502 x 302 x 50 mm, density 0.0226 g/cm^3
2	Gray foam	ESPCIN	Dimensions 502 x 302 x 50 mm, density 0.0184 g/cm^3
3	Alveolar black foam	ESPPRE	Dimensions 421 x 232 x 45 mm, mass 65.75 g
4	Alveolar white foam	ESPBRA	Dimensions 351 x 310 x 45 mm, mass 57.73 g
5	Bubble wrap	PLABOL	Bubble diameter 10 mm, mass 84.67 g
6	Black rubber	BORPRE	Section dimensions 25 x 12 mm, density 0.4889 g/cm^3
7	Damper	VIBSTO	Damper Vibra-stop VS.01, diameter 20 mm, capacity 10 kg
8	Small spring	MOLAPQ	Thickness 1.8 mm, external diameter 18.6 mm, n^o coils 2.5, mass 2.53 g, ref. 2604617006720
9	Big spring	MOLAGD	Thickness 1.7 mm, external diameter 17.5 mm, n^o coils 7, mass 5.21 g, ref. 1604616018
10	Box suspended nylon	CAVNYL	Box suspended by 2 nylon threads (0.5 mm, 32 kg) on the easel
11	Box suspended elastic	CAVELA	Box suspended by an elastic tube. ref. 202 (external diam. 10 mm e internal diam. 5 mm)

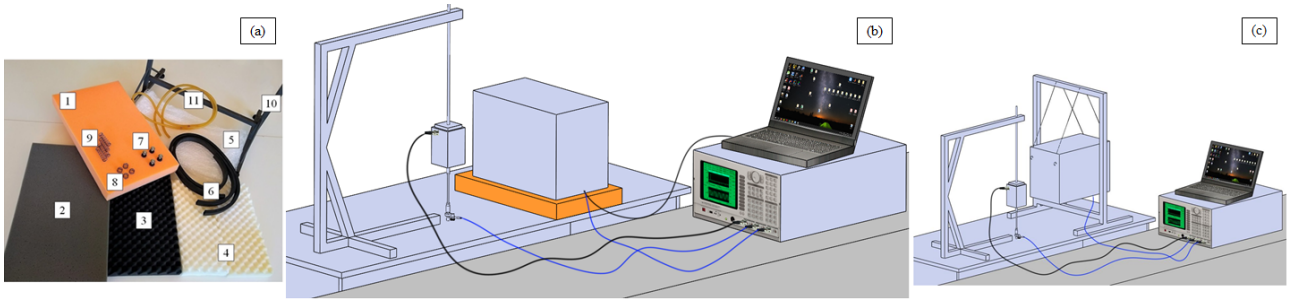

Figure 3. Shock absorbers (a); Experimental setup - Transmissibility and DLS test (b); Prototype suspended from the easel (c).

Considering that one of the objectives of this work is the reduction of external vibration interference in the biospeckle laser technique proposing the use of a mechanical isolator, DLS tests were also performed and analyzed along with the transmissibility curves for each shock absorber. The experimental procedure followed the same protocol as the test performed with the prototype on the table without shock absorbers. The excitations were promoted by the shaker on the table in the vertical direction at frequencies of 5, 15, 25, 42, 60, 112, 470, 800 Hz, at three different levels of intensity (amplitude): 40, 70 and 100 mVpk. For each of these combined conditions, while the table was excited at a certain frequency and amplitude, 4 captures of 128 images were taken at a speed of 15 fps, to calculate the AVD. The final AVD was calculated through the average of the 4 values obtained in these 4 captures. The experimental configuration used for the tests can be seen in Figure 3a. The orange element, where the box is on, represents the 11 shock absorbers used in this work.

3. RESULTS

3.1 Prototype natural frequencies

The FRF curves obtained for the respective axes can be seen in Figure 4. The occurrence of more visible peaks between the 5 accelerometers can be better observed at frequencies up to approximately 350 Hz, after that, each accelerometer

assumes a behavior relatively more independent from the others. In the 0-200 Hz range, it can be better observed the occurrence of concomitant peaks not only between the five accelerometers in a given axis but also peaks between the axes. The frequencies at which these peaks occur represent the prototype's natural frequencies.

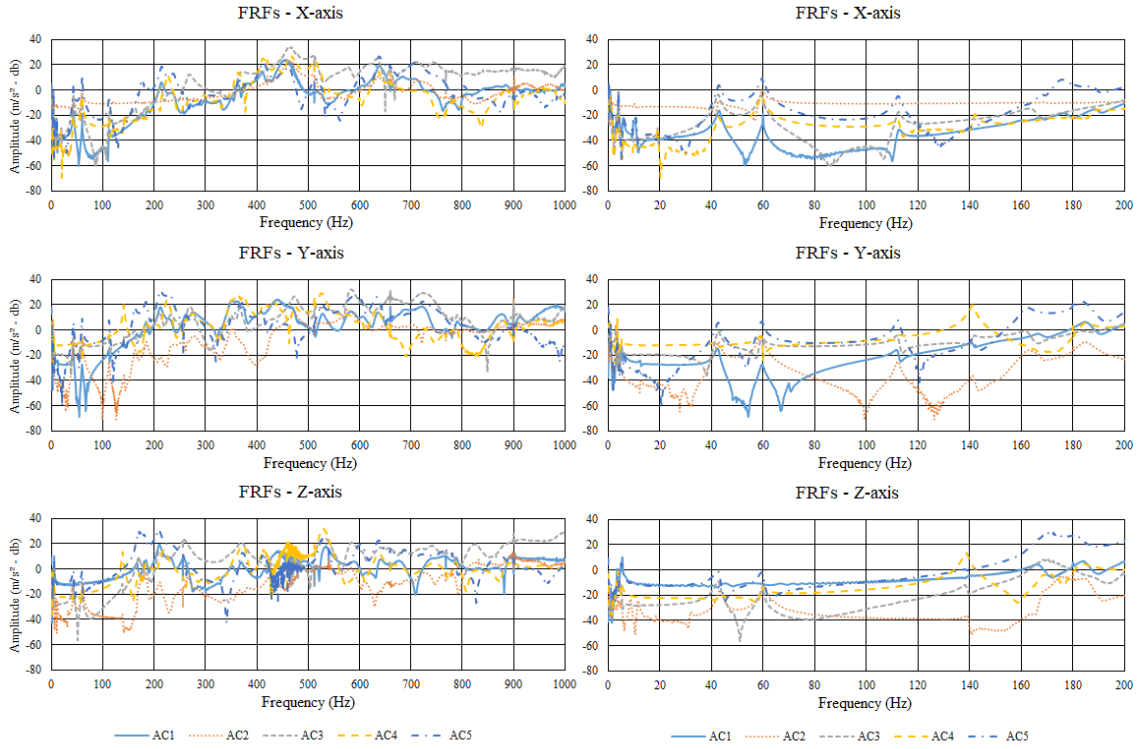

Figure 4. FRFs per axis - 0-1000 Hz and 0-200 Hz.

As the structure of the prototype is complex, composed of several support elements, fixation, and devices made of different materials (see Figure 1), for excitations at higher frequencies, where the vibrating modes are generally more complex, at first glance, there is a dissipation of excitation energy throughout the prototype structure, added to a portion of noise and non-linearity, hence the difficulty in finding more salient peaks at higher frequencies.

The observed natural frequencies on the three axes are:

X-axis → 4; 6; 9.75; 19.25; 42; 60; 112; 215; 365; 412; 470; 510; 640; 710; 725; 790; 880 Hz.

Y-axis → 3.5; 5.2; 12.5; 42; 60; 112; 142; 186; 214; 350; 471; 529; 580; 635 Hz.

Z-axis → 3.7; 5.2; 42; 60; 139; 175; 210; 265; 370; 415; 530; 638 Hz.

Values up to 3 Hz were not considered in the analysis due to experimental limitations and equipment sensitivity. The first natural frequency of each axis (4, 3.5, and 3.7 Hz) regards the rigid body, resulting from free-free mounting, and the others, flexible body. As can be seen in Figure 4, some natural frequencies presented sharper peaks than others; 42 Hz and 60 Hz, for example, appear on the 3 axes for the 5 accelerometers. Others, also in the 3 axes, x, y and z, respectively, appear very close: 4, 3.5 and 3.7; 6, 5.2 and 5.2; 215, 214 and 210; 365, 350 and 370; 510, 529 and 530; 640, 635 and 638 Hz. Figure 5a represents the mean of the amplitude values obtained in the FRFs of the 5 accelerometers, for each axis. It is possible to observe more clearly the natural frequencies that are predominant in the 3 axes.

3.2 AVD vs Frequency

Graphs representing the behavior of the AVD were generated when the suspended prototype is directly excited at punctual frequencies from 0 to 1000 Hz, in the three axes. For better visualization and presentation of these same data, they were displayed in two more intervals, of low and medium frequencies: 0 to 50 and 0 to 400 Hz (Figure 5b). It can be seen that the DLS technique was more sensitive to excitations at low frequencies than to high frequencies, presenting maximum values at excitations close to 5 Hz. There was a more accentuated drop in the index AVD, in the 3 axes, at excitations close to 210 Hz, signaling a system response to the resonance region close to this frequency, as can be seen in Figures 4 and 5a. This drop in the AVD may be related to the capacity of the camera. As its capture speed is 15 fps (15 Hz), and the resonance in the 210 Hz range promotes a high excitation of the set (as well as in the resonances at 42 and 60 Hz), the camera was not able to capture the phenomenon with enough speed, and the resulting speckle pattern image was blurry. Therefore, the grains in the pattern were poorly defined and the AVD decreased. For the other frequency ranges,

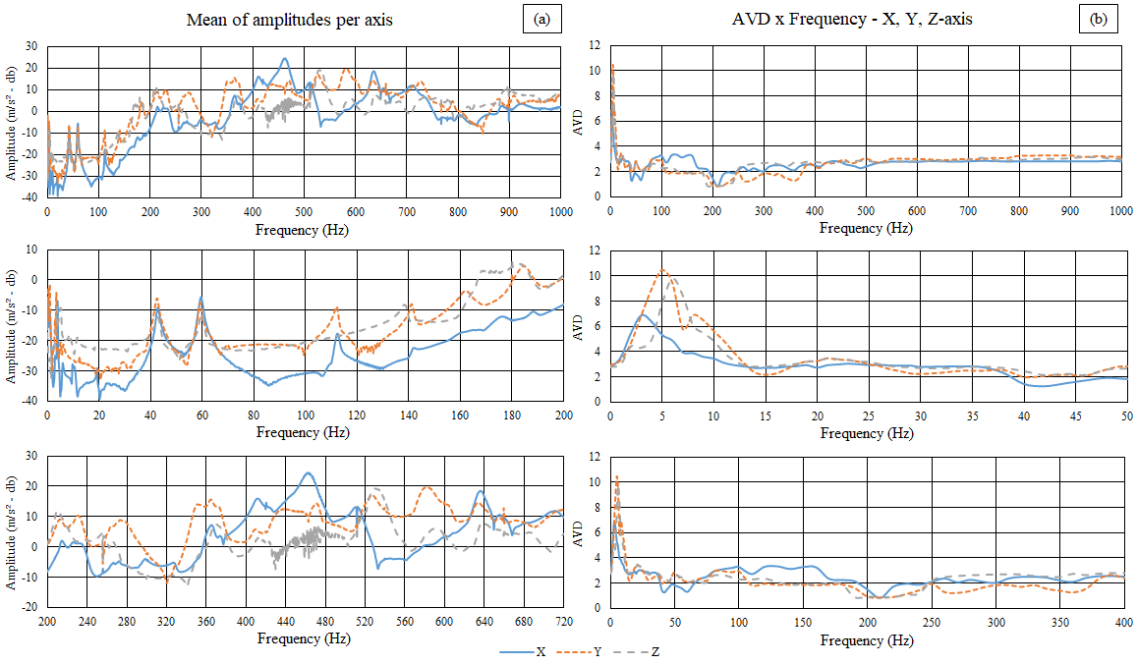

Figure 5. Mean of amplitudes per axis (a); AVD x Frequency (b).

there was little variation, especially at frequencies above 400 Hz. These results attest to the influence of vibration on the AVD, demanding the use of a vibration isolator to mitigate this effect.

As the camera's capture speed is 15 fps, it is inferred that this is the main reason for the evident greater sensitivity of the AVD index to low frequencies, a phenomenon that would be observed even if there were no natural frequencies in this range. At other more notable natural frequencies like 42, 60, and 112 Hz for example, the variation in the AVD observed is a little smaller, albeit notable. For natural frequencies that occurred at values above 250 Hz, the influence of resonance on the DLS was increasingly smaller. This may be because the prototype's housing and structure absorb such vibrations, in addition to being a frequency well above the camera's capture rate. These results suggest that, when designing a vibration isolator for a portable device capable of performing biospeckle laser analysis, the frequency ranges to be isolated should be the lowest, since high frequencies are easier to be filtered and the images captured for DLS analysis are typically performed at a speed of 10 to 15 fps.

3.3 Transmissibility

The results of the transmissibility tests can be seen in their entirety in Figure 6a. Also included for comparison is the transmissibility result for the prototype under the table without any vibration isolating device, where the code can be seen in the graph as SEMAMO (no damping). It was observed that for values above 60 Hz there is no amplification of the response signal, that is, the transmissibility is less than 1. For most isolation materials, it was observed that at lower frequencies, from 0 to 9 Hz approximately, there is a transient period where random oscillations occurred for transmissibility values around 0.1 and 1, due to this, it was not possible to obtain precise information in this frequency range. For better visualization and interpretation of the results, the transmissibility graphs were divided into 3 domains: 1) foams; 2) rubber, vibra-stop, and springs; 3) bubble wrap and easels.

For the foams, Figure 6b, it could be seen that ESPBRA was the one with the best vibration isolation conditions. With a curve similar to ESPPRE, its first resonance peak occurred at the lowest frequency compared to the others, 16.75 Hz. Its curve also presented the lowest transmissibility values, indicating greater efficiency in isolating vibrations. Followed by ESPPRE, which is also alveolar and has a resonance peak at 18.5 Hz. ESPCIN and ESPLAR had a similar behavior due to the small density difference between the two, with a resonance peak of 26.75 Hz for ESPLAR and 27 Hz for ESPCIN, which proved to be more efficient in isolating higher frequencies (from 130 Hz). For the other frequencies, ESPLAR, despite the second resonance peak at 60 Hz, was slightly more efficient than ESPCIN in the range of 65 to 130 Hz. It is interesting to note that from 30 to 55 Hz, the transmissibility behavior of all foams, as well as the behavior without isolator, were similar, indicating that, for this frequency range, insulation with foams similar to those studied would not be the best choice.

Regarding the graph in Figure 6c, a lower isolation efficiency was observed for the elements with greater rigidity (harder), such as BORPRE and VIBSTO, where the resonance peak occurred close to both: 29.5 Hz and 30 Hz, respectively. The peak amplitude of VIBSTOP was the highest among all tested elements, indicating a higher amplification

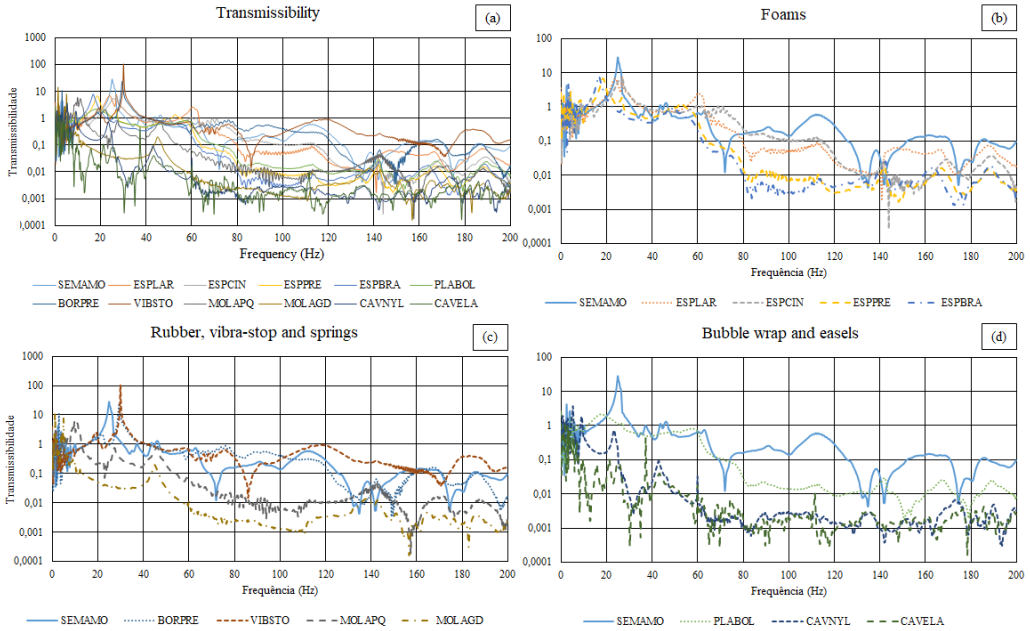

Figure 6. Transmissibility.

even than SEMAMO, at this resonance. BORPRE exhibited behavior similar to VIBSTOP up to 80 Hz, and for higher frequencies, it was more efficient in isolation. Both springs proved to be far superior to the other components. With also similar curves, MOLAGD presented better transmissibility results compared to MOLAPQ. For frequencies above 6 Hz, MOLAGD did not present any amplification in the response signal ($T_d > 1$), and as at low frequencies (up to $\approx$ 9 Hz) there is a transience in the signal, apparently due to the range of response of transducers and the experimental configuration, transmissibility values observed in this range may be even lower, showing the potential of MOLAGD concerning other devices. The first resonance peak presented in MOLAPQ was at 9.75 Hz, and the peak in MOLAGD was at 5 Hz.

Among the range of insulators tested observed in Figure 6d, it is important to point out that the tests carried out with the box suspended by the trestle through nylon and elastic tube (CAVNYL and CAVELA) are purely experimental, simulating conditions of ideal insulation, that is, its eventual evolution for practical application in a portable SLD device is more difficult. PLABOL presented excellent insulation characteristics, with a resonance peak at 17.75 Hz occurring with a low magnitude, compared to the other insulators mentioned above. From this peak, the transmissibility remained below 1, indicating good isolation efficiency. Efficiency that would be even better if the transmissibility were lower for frequency values between 20 and 60 Hz. The transmissibility results for CAVNYL and CAVELA were the best, as expected. CAVELA, compared to CAVNYL, obtained better results at low frequencies (up to $\approx$ 35 Hz) due to the elastic tube being less rigid than nylon thread. For higher frequencies, both devices behaved similarly, obtaining the lowest attenuation levels among all, in the range of T_d = 0.001.

3.4 AVD x Frequency results with vibration isolators

Once the transmissibility curves for each insulating element were established, it was possible to determine which element more efficiently attenuates the vibration promoted by the shaker. However, it was necessary to investigate with what intensity this attenuation occurs in the biospeckle laser technique. The results obtained in the experiment described in Section 2.5 are expressed in Figure 7. Twelve graphs were plotted, one for each experimental condition. In them, it was possible to observe the variation of the AVD, for each excited frequency, in the three different studied amplitudes.

It was observed that in the domain of foams there are two different formats, one in the conventional bespoke format (ESPLAR and ESPCIN) and the other in the alveolar format (ESPPRE and ESPBRA). Foams with an alveolar profile, in general, presented AVD results with less variability when compared to those with a conventional profile, indicating better vibration absorption. This result could also be observed in the transmissibility curves, Figure 6, where ESPPRE and ESPBRA also obtained better results. It was found that there is a great influence of the 42 Hz frequency in foam absorbers. The influence proved to be greater than in SEMAMO, where there is no damping device. This fact occurred because in addition to 42 Hz being an expressive natural frequency of the prototype it is also close to the table's natural frequency, which could amplify the transmissibility levels and explain why the values of T_d between 40 to 60 Hz in Figure 6b remained relatively high. The variation of AVD values for ESPCIN was lower than for ESPLAR, which has a density 23% higher. ESPPRE and ESPBRA showed similar behaviors.

The results of BORPRE and VIBSTO were inferior to SEMAMO, indicating that they are not an option for mechanical

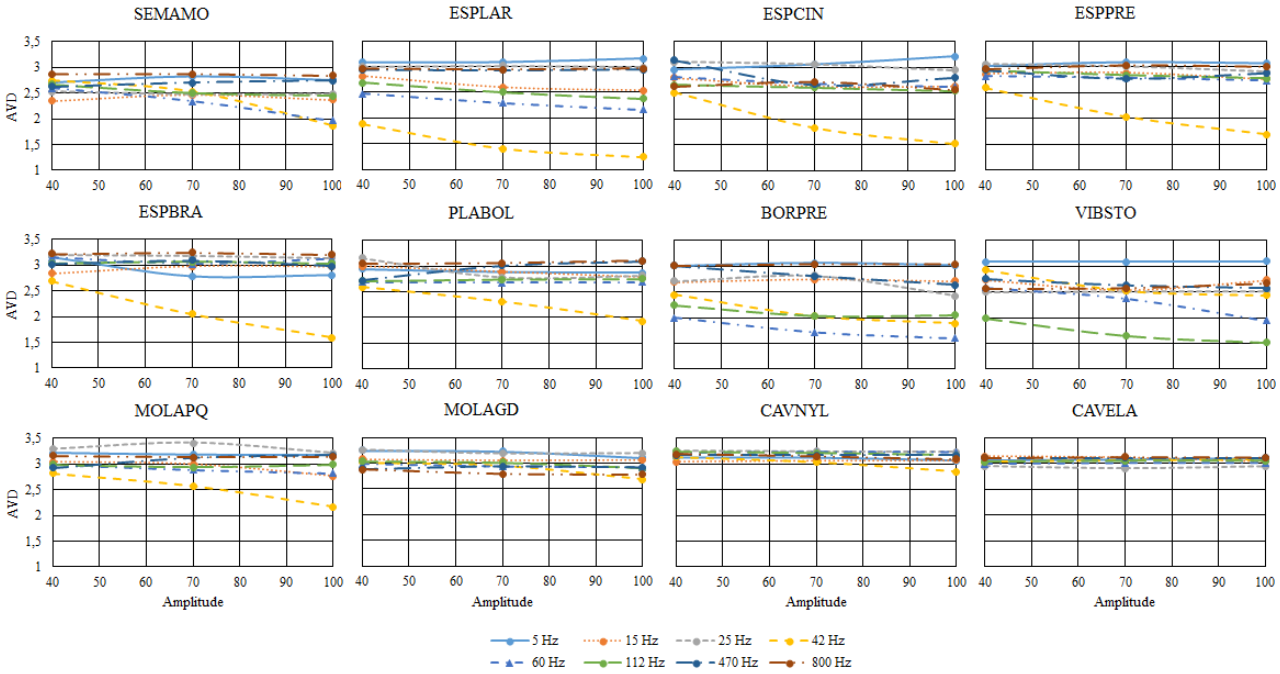

Figure 7. AVD vs Frequency - Amplitude.

dampers in a DLS prototype. They presented great variability, agreeing with their transmissibility curves, which exhibited inefficient responses to reduce vibration. PLABOL proved to be an interesting result, similar to that of ESPPRE and ESPBRA, however, it was also strongly influenced by the natural frequency of 42 Hz.

Superior results, in agreement with the transmissibility results, were achieved by the spring and easels isolators. CAVNYL and CAVELA, which in this work reproduced the ideal isolation conditions, as expected, obtained minimal and insignificant variations in the AVD index. CAVNYL exhibited a slightly greater variation than CAVELA and, unlike CAVELA, it was slightly sensitive to the 42 Hz frequency when the system was excited at the maximum amplitude of 100 mVpk. These insulators had the lowest natural frequencies, as can be seen in Figure 6d, justifying the higher and better attenuation range. MOLAGD's vibration isolation performance, as well as in the Transmissibility test, Figure 6c, was superior to MOLAPQ and other absorbers devices, managing to filter the frequency that most affected the AVD index in these tests, that of 42 Hz.

4. CONCLUSION

In this work, a portable configuration for laser biospeckle analysis was proposed. The natural frequencies of the proposed configuration were obtained and also it was discovered how the AVD index behaves when excited at these and other frequencies, in a range from 0 to 1000 Hz. It was found that the AVD is more sensitive to low frequencies, in the region around 5 Hz For higher frequencies, the AVD proved to be less sensitive, presenting values even below the reference value, in regions of high resonance, such as close to 42, 60 and 210 Hz, however, these values do not indicate low activity. In the transmissibility tests, which analyzed the transmittance of vibration from the table to the prototype and 11 more isolating devices, it was also found that for high frequencies the filtering of vibrations by the system is greater, and the transmissibility lower. A result that was consistent with the theory.

The AVD results were, in general, in agreement with the transmissibility results, that is, the configurations with the shock absorbers that presented low vibration transmissibility also presented less variability in the DLS index. The 42 Hz frequency proved to be quite influential on the index for most isolators, as it is one of the prototype's resonance frequencies and also being close to the resonance frequency of the table where it was set up.

Among the absorbers, the spring with the lowest stiffness, MOLAGD, was the one with the best vibration isolation characteristics, a result validated by the AVD. Furthermore, taking into account the constructive issue, the spring also has the advantage of being easily installed in the base of the prototype.

5. ACKNOWLEDGEMENTS

This study was financed in part by the Coordenação de Aperfeiçoamento de Pessoal de Nível Superior – Brasil (CAPES) – Finance Code 001.

6. REFERENCES

Aizu, Y. and Asakura, T., 1991. "Bio-speckle phenomena and their application to the evaluation of blood flow". *Optics Laser Technology*, Vol. 23, No. 4, pp. 205 – 219. ISSN 0030-3992.

Ansari, M.Z. and Nirala, A., 2013. "Assessment of bio-activity using the methods of inertia moment and absolute value of the differences". *Optik - International Journal for Light and Electron Optics*, Vol. 124, No. 6, pp. 512 – 516.

Avitabile, P., 2018. *Modal Testing: A Practitioner's Guide*. Wiley, New Jersey. ISBN 9781119222897.

Balbinot, A., 2001. *Caracterização dos níveis de vibração em motoristas de ônibus: um enfoque no conforto e na saúde (in Portuguese)*. Ph.D. thesis, Graduate Program in Mechanical Engineering, Federal University of Rio Grande do Sul, Porto Alegre, Brazil.

Becker, T., 2006. *Desenvolvimento de uma mesa vibratória para estudos sobre vibração no corpo humano, medições em um grupo de motoristas e ajuste de um modelo biodinâmico (in Portuguese)*. Ph.D. thesis, Graduate Program in Mechanical Engineering, Federal University of Rio Grande do Sul, Porto Alegre, Brazil.

Blotta, E., Ballarin, V. and Rabal, H., 2009. "Decomposition of biospeckle signals through granulometric size distribution". *Opt. Lett.*, Vol. 34, No. 8, pp. 1201–1203. doi:10.1364/OL.34.001201.

Braga, R.A., Borém, F.M., Rabelo, G.F., Fabbro, I.M.D., Arizaga, R.A., Rabal, H.J. and Trivi, M., 2001. "Seeds analysis using bio-speckle". *Proceedings of SPIE - The International Society for Optical Engineering*, Vol. 4419, pp. 34–37.

Braga, R.A., Rivera, F.P. and Moreira, J., 2016. *A Practical Guide to Biospeckle Laser Analysis: Theory and Software*. UFLA, Lavras. ISBN 9-788581-270517.

Carvalho, P.H., Barreto, J.B., Braga, R.A. and Rabelo, G.F., 2009. "Motility parameters assessment of bovine frozen semen by biospeckle laser (bsl) system". *Biosystems Engineering*, Vol. 102, No. 1, pp. 31 – 35. ISSN 1537-5110.

Chaves, M.J., 2011. *Desenvolvimento de uma metodologia para análise do biospeckle laser com portabilidade, acessibilidade e robustez (in Portuguese)*. Master's thesis, Graduate Program in Systems and Automation Engineering, Federal University of Lavras, Lavras, Brazil.

da Silva, E.R., 2007. *Study of biospeckle properties and its applications (in Portuguese)*. Master's thesis, Graduate Program in Physics, University of Sao Paulo, São Paulo, Brazil.

de Castro, D.B., 2020. *Experimental research of the mechanical vibration effects in the biospeckle laser technique for portable equipment application (in Portuguese)*. Master's thesis, Graduate Program in Systems and Automation Engineering, Federal University of Lavras, Lavras, Brazil.

Fracarolli, J.A., 2011. *Application of the laser biospeckle in evaluation ipê-roxo (Tabebuia heptaphylla) (Vellozo) Toledo (in Portuguese)*. Master's thesis, Graduate Program in Agricultural Engineering, Campinas State University, Campinas, Brazil.

Inman, D.J., 2007. *Engineering Vibration*. Pearson Education, New Jersey, 3rd edition. ISBN 0132281732.

Junior, R.A.B., Silva, B.O., Rabelo, G., Costa], R.M., Enes, A.M., Cap, N., Rabal, H., Arizaga, R., Trivi, M. and Horgan, G., 2007. "Reliability of biospeckle image analysis". *Optics and Lasers in Engineering*, Vol. 45, No. 3, pp. 390 – 395.

Lopes, H., dos Santos, J.A., Moreno-García, P. and Monteiro, J., 2017. "Influence of shearing amount and vibration amplitude on noise in shearography". *Procedia Structural Integrity*, Vol. 5, pp. 1205 – 1212. ISSN 2452-3216. 2nd International Conference on Structural Integrity, ICSI 2017, 4-7 September 2017, Funchal, Madeira, Portugal.

McMahon, G., 2008. *Analytical Instrumentation: A Guide to Laboratory, Portable and Miniaturized Instruments*. Wiley.

Pomarico, J., Di Rocco, H., Alvarez, L., Lanusse, C., Mottier, L., Saumell, C., Arizaga, R., Rabal, H. and Trivi, M., 2005. "Speckle interferometry applied to pharmacodynamic studies: Evaluation of parasite motility". *European biophysics journal : EBJ*, Vol. 33, pp. 694–9. doi:10.1007/s00249-004-0413-4.

Porcu, M., Patteri, D., Melis, S. and Aymerich, F., 2019. "Effectiveness of the frf curvature technique for structural health monitoring". *Construction and Building Materials*, Vol. 226, pp. 173 – 187. ISSN 0950-0618.

Pra, A.L.D., Passoni, L.I. and Rabal, H., 2009. "Evaluation of laser dynamic speckle signals applying granular computing". *Signal Processing*, Vol. 89, No. 3, pp. 266 – 274. ISSN 0165-1684.

Rabal, H. and Braga, R.A., 2008. *Dynamic laser speckle and applications*. CRC Press, New York.

Rao, S.S., 2010. *Mechanical Vibrations*. Pearson Education, New Jersey, 5th edition. ISBN 9780132128193.

SRS, 2017. "Operating manual and programming reference". STANFORD RESEARCH SYSTEMS, Model SR785 - Dynamic Signal Analyser. 1290-D Reamwood Avenue Sunnyvale, CA, United States of America.

Zhong, X., Wang, X., Cooley, N., Farrell, P. and Moran, B., 2013. "Dynamic laser speckle analysis via normal vector space statistics". *Optics Communications*, Vol. 305, pp. 27 – 35. ISSN 0030-4018.

7. RESPONSIBILITY NOTICE

The authors are solely responsible for the printed material included in this paper.